Aharonov–Bohm differential conductance modulation in defective metallic single-walled carbon nanotubes

2008 J. Phys.: Condens. Matter 20 075227

(http://iopscience.iop.org/0953-8984/20/7/075227)

IOP PUBLISHING JOURNAL OF PHYSICS: CONDENSED MATTER

J. Phys.: Condens. Matter **20** (2008) 075227 (7pp) doi:10.1088/0953-8984/20/7/075227

Aharonov–Bohm differential conductance modulation in defective metallic single-walled carbon nanotubes

Mehran Bagheri

Physics Department, Shahid Beheshti University, Evin, Tehran 19839, Iran

E-mail: mh-bagheri@cc.sbu.ac.ir

Received 12 June 2007, in final form 7 December 2007
Published 31 January 2008
Online at stacks.iop.org/JPhysCM/20/075227

Abstract

Using a perturbative approach, the effects of the energy gap induced by the Aharonov–Bohm (AB) flux on the transport properties of defective metallic single-walled carbon nanotubes (MSWCNTs) are investigated. The electronic waves scattered back and forth by a pair of impurities give rise to Fabry–Perot oscillations which constitutes a coherent backscattering interference pattern (CBSIP). It is shown that the CBSIP can be aperiodically modulated by applying a magnetic field parallel to the nanotube axis. In fact, the AB-flux brings this CBSIP under control by an additional phase shift. As a consequence, the extrema as well as zeros of the CBSIP are located at the irrational fractions of the quantity $\Phi_\rho = \Phi/\Phi_0$, where Φ is the flux piercing the nanotube cross section and $\Phi_0 = h/e$ is the magnetic quantum flux. Indeed, the spacing between two adjacent extrema in the magneto-differential conductance (MDC) profile is decreased with increasing magnetic field. The faster and higher and slower and shorter variations are then obtained by metallic zigzag and armchair nanotubes, respectively. Such results lead to the proposal that defective metallic nanotubes could be used as magneto-conductance switching devices based on the AB effect.

(Some figures in this article are in colour only in the electronic version)

1. Introduction

Due to their quasi-one-dimensional structure and intriguing electronic properties, carbon nanotubes have attracted an increasing amount of attention [1]. Carbon nanotubes are tubular nano-objects which can be thought of as graphenes wrapped onto a seamless cylinder. Depending sensitively on the wrapping vector, a nanotube may be either a one-dimensional (1D) metal with a finite density of states at the Fermi energy or a semiconductor with a gap. In particular, because of the 1D nature of their electronic conduction bands near the Fermi energy, metallic single-walled nanotubes constitute a nearly perfect realization of 1D quantum wires [2–5].

The investigation of quantum transport in carbon nanotubes is expected to lead to unprecedented potential applications for the development of nanoelectronic devices. They can be applied as conducting quantum wires [5, 6], single-electron tunneling transistors [7, 8], field-effect transistors [9], and spin-electronic devices [10]. Theoretical calculations based on the Landauer–Bütticker formalism [11, 12] predict conductance quantization for a perfect metallic nanotube for the case of ideal contacts. The maximum value of the conductance near the Fermi energy reaches $2G_0$, where $G_0 = 2e^2/h$ is the conductance quantum [13]. However, in contrast to a pristine nanotube, several theoretical works [14–20] and experimental evidence [21–24] have shown that in the presence of disorders coming from various sources like chemical impurities, topological defects [25], and vacancies this quantized conductance of nanotubes does not follow the aforesaid results. In practise these imperfections are unavoidable when manipulating nanotubes into devices and induce departure from ballistic transport, and yet preserve quantum interference effects which can be profoundly affected by magnetic fields.

Owing to the decoherence, the quantum corrections to the classical conductance of a device are usually negligible in macroscopic systems at the room temperature. In mesoscopic systems at low temperatures, however, the

quantum mechanical coherency becomes more important because the phase coherence length l_ϕ increases with decreasing temperature. When the coherence length l_ϕ exceeds the elastic mean free path l_m, scattering on different impurities can interfere. Several QI modifications are: (1) the WL correction, which originates when pairs of time-reversed paths in a diffusive sample interfere constructively in the zero magnetic field. This interference enhances (reduces) the probability of electronic backscattering, decreasing (increasing) the conductance of the sample [26]. (2) The AB and Altshuler–Aronov–Spivak (AAS) oscillations. The AAS effect is actually the same WL correction embracing a magnetic field [27–29]. As the magnetic field is increased, the AB phase eliminates the WL constructive interference, leading to magneto-conductance. (3) Universal conductance fluctuations (UCF), which means that the conductance fluctuations are independent of the details of the conductor.

Furthermore, one of the unique properties of carbon nanotubes is that their metallicity can be controlled by an external magnetic field applied parallel to the nanotube axis. This magnetic field gives rise to a periodic energy gap at the charge neutrality point (CNP), where the bonding and antibonding bands are crossed. When the cross section of a nanotube is pierced by the magnetic field, the electronic wavefunctions acquire an additional phase $2\pi\Phi/\Phi_0$. Thus, metallic nanotubes can be made semiconducting and vice versa. Over the past few years, remarkable efforts have been undertaken to discover the effects of a magnetic field on the band structure of nanotubes [30–43].

Following our previous paper [44], in which a perturbative approach is well developed to include effects of the band structure and impurity on the transport characteristics of metallic nanotubes, the current work concentrates on elucidating the influence of the AB-flux [45] on the differential conductance (DC). The reason for this attempt is to study how the magnetic field dependence of the band structure of the nanotube influences the DC. This may provide us with the possibility of fabricating magneto-conductance switching devices based on the AB effect in defective metallic nanotubes. It is shown that, for a couple of impurities, the nanotube behaves like a Fabry–Perot electron resonator [53, 54] and the coherent backscattering interference pattern (CBSIP) resulting from the Fabry–Perot oscillations is aperiodically modulated in the presence of the AB-flux. Aperiodicity means that no specific magnetic flux periodicity is found in the MDC profile. Further, extrema as well as zeros of the MDC are positioned at irrational fractions of the magnetic flux with a spacing which is decreased by increasing the magnetic field.

The paper is organized as follows. In section 2, the model of [44] is developed to include the AB-flux. In section 3, we discuss the CBSIP in the presence of the AB-flux both for a single impurity and for a couple of impurities.

2. Theoretical model

We address a defective metallic single-walled carbon nanotube (MSWCNT) in the presence of an axial electric and magnetic field. A full description of the model in the absence of the magnetic field can be found in [44]. Here, we just add the AB-flux in its band structure, so the Hamiltonian of the whole system is given by

$$\hat{\mathcal{H}}(\Phi_\rho) = \hat{\mathcal{H}}_{\rm tube}(\Phi_\rho) + \hat{\mathcal{H}}_{\rm sd} + \hat{\mathcal{H}}_{\rm imp}. \tag{1}$$

In the above equation the first term, describing the kinetic energy of electrons for a perfect nanotube, is given by [44, 46]

$$\hat{\mathcal{H}}_{\rm tube}(\Phi_\rho) = \sum_{\alpha=\pm}\sum_{q=1}^{N_t/2}\sum_{k\in}^{\rm FBZ} \mathcal{E}^{\alpha}_{q+\Phi_\rho}(k)\hat{C}^{\dagger\alpha}_q(k)\hat{C}^{\alpha}_q(k). \tag{2}$$

In the presence of a uniform magnetic field $\vec{B}$ parallel to the nanotube axis, the wrapping modes are modified according to $q/r_t \to q/r_t + \Phi_\rho/r_t$ [31], so the magnetic field dependent band structure $\mathcal{E}^{\pm}_{q+\Phi_\rho}(k)$ is [44]

$$\begin{aligned}\frac{\mathcal{E}^{\pm}_{q+\Phi_\rho}(k)}{\gamma_0} &= \pm\left\{1+4\cos\left[\frac{\sqrt{3}}{2}a_{\rm cc}\left(\frac{1}{r_t}[q+\Phi_\rho]\sin\omega + k\cos\omega\right)\right]\right.\\ &\quad\times\cos\left[\frac{3}{2}a_{\rm cc}\left(\frac{1}{r_t}[q+\Phi_\rho]\cos\omega - k\sin\omega\right)\right]\\ &\quad\left.+4\cos^2\left[\frac{\sqrt{3}}{2}a_{\rm cc}\left(\frac{1}{r_t}[q+\Phi_\rho]\sin\omega + k\cos\omega\right)\right]\right\}^{\frac{1}{2}},\end{aligned} \tag{3}$$

where operators $\hat{C}^{\dagger\pm}_q(k)$ and $\hat{C}^{\pm}_q(k)$ create and destroy electrons in the orbital with energy $\mathcal{E}^{\pm}_{q+\Phi_\rho}(k)$, respectively. The + and − signs correspond to the conduction and valence band, respectively. Good quantum numbers of electron states are (q,k) where $q = 1,\ldots,N_t/2$ and $k \in (-\pi/T,\pi/T)$. The quantities N_t, $\mathcal{N} = N_t/2$, T, r_t, $a_{\rm cc} \simeq 1.44$ Å, and $\gamma_0 \simeq 3.0$ eV are the number of carbon atoms in the nanotube unit cell, the number of graphene unit cells in a given nanotube unit cell, the length of the translation vector, the nanotube radius, the C–C bond length, and the nearest-neighbor overlap integral energy, respectively. Also, $\omega = \pi/6 - \theta$ where θ is the chiral angel of the nanotube whose value for the armchair and zigzag nanotube is $\pi/6$ and 0, respectively. It is assumed that the on-site energy is zero and the Fermi energy remains unchanged at the CNP. In zero magnetic field, all metallic linear bands cross the undoped Fermi level either degenerated at $k_{\rm F} = 0$ (metallic zigzag) or separated at $k_{\rm F} = \pm 2\pi/3T$ (armchair) in the first Brillouin zone (FBZ). Φ_ρ equals Φ/Φ_0, with $\Phi = \pi r_t^2 B$. When Φ_ρ becomes an integer, the AB-flux is canceled by q. This means that the gap induced by the magnetic field oscillates periodically and can be obtained by the expression $\Delta_g(\Phi_\rho) = 2\min\{|\mathcal{E}^{+}_{q+\Phi_\rho}(k)|\}$ (see figure 1(a)). Lu [42] has shown that, for metallic nanotubes, the energy gap induced by an axial magnetic field is expressed by

$$\Delta_g(\Phi_\rho) = \begin{cases} 3\Delta_0\Phi_\rho, & \text{if } 0 \leqslant \Phi_\rho \leqslant \frac{1}{2} \\ 3\Delta_0|1-\Phi_\rho|, & \text{if } \frac{1}{2} \leqslant \Phi_\rho \leqslant 1, \end{cases} \tag{4}$$

where $\Delta_0 = \gamma_0 a_{\rm cc}/r_t$ defines a characteristic energy associated with the nanotube. Note that the expression $\mathcal{E}^{\pm}_{q+\Phi_\rho}(k) = \pm\gamma_0\sin[\pi(q+\Phi_\rho)/n]$ gives van Hove singularity positions.

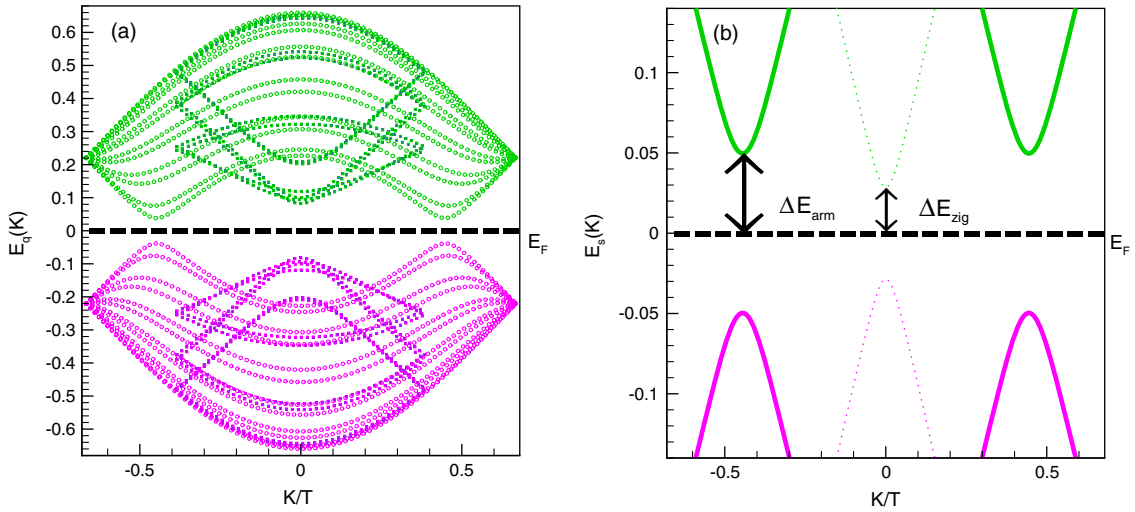

Figure 1. The energy dispersion relation for subbands of armchair and metallic zigzag nanotubes in the presence of an axial magnetic field. (a) A multiband model, coming from evaluating equation (3) in the presence of a 1000 T magnetic field pointing along its axis, for the (6, 6) armchair (circle) and (6, 0) zigzag (square) nanotubes. The nanotube now has a finite subband-gap $\Delta_g(\Phi_\rho)$ expressed by equation (4), and all degenerate levels have been split. Antibonding bands (green, $E_q(k) > 0$) are symmetric to the bonding bands (purple, $E_q(k) < 0$). (b) A two-band model, which comes from evaluating equation (5) ($E_s(k)$ with $s = 1$) in the presence of a 10 mT magnetic field pointing along its axis, includes the (6, 6) armchair (solid line) and (6, 0) zigzag (dotted) nanotubes. The subband-gap is now expressed by $\Delta_g(\Phi_\rho) = 3\Delta_0\Phi_\rho$. The electron scattering processes change electrons from right moving to left moving leading to electrical resistance. Generally, both intrasubband and intersubband scattering events are likely. Energies are scaled in Rydberg and lengths in the Bohr radius.

Further, for later calculations we have exploited the corresponding Bloch states of an isolated nanotube previously derived in [44].

To consider the magneto-transport properties of the nanotube near the Fermi level we adopt the light-cone approximation of the dispersion relation of equation (3) which provides us with a simple formula of the sth 1D subband around k_F. Thus, equation (3) reduces to [31]

$$\frac{\mathcal{E}^{\pm}_{s+\Phi_\rho}(k)}{\gamma_0} = \pm\frac{3a_{cc}}{2}\left[\left(\frac{s-1}{r_t}+\frac{\Phi_\rho}{r_t}\right)^2 + (k \mp k_F)^2\right]^{1/2}, \tag{5}$$

where $s = 1, \ldots, N_t/2$. For the lowest lying subband, with $s = 1$ around $k = \pm k_F$, the energy band gap in the absence of a magnetic field is zero. Using equation (5) one obtains $\Delta_g(\Phi_\rho) = 3\Delta_0\Phi_\rho$. As the field strength increases the line through the Fermi energy at zero magnetic field is shifted away further from the CNPs thus given rise to an increasing energy gap. It is also worth mentioning that the quantity $\mu_{orb} = ev_F r_t/2$, with $v_F = 3\gamma_0 a_{cc}/2\hbar \approx 10^6$ m s^{-1}, is the magnetic moment of an electron traveling in a loop of radius r_t with velocity v_F. Changes in the energy of electron states can be described by the interaction of this orbital magnetic moment with an axial magnetic field. A magnetic field parallel to the nanotube axis is predicted to shift the energy of these states by $\Delta E = -\vec{\mu}_{orb}\cdot\vec{B} = \pm ev_F r_t B/2 = \pm 3\Delta_0\Phi_\rho/2$ (see figure 1(b)).

Furthermore, the second and third terms in equation (1) are, respectively, the Hamiltonian of non-interacting electrons under the external source–drain voltage V_{sd} and the Hamiltonian of the interaction of electrons with impurities [47–49] like those presented in [44]. Eventually, upon substituting q in equation (20) of [44] by $q + \Phi_\rho$, we obtain the dimensionless form of the MDC at zero temperature as follows:

$$\begin{aligned}\frac{G^{\alpha\alpha}_{imp}[V_{sd}, \mathcal{E}_F(0), \Phi_\rho]}{G_0} &= \frac{\pi^2}{2}\sum_{q,q'=1}^{N_t/2}\sum_{k,k'\in\xi,\eta=1}^{FBZ}\sum^{r} J^{qq'}_{\xi,\alpha\alpha}(k,k')J^{q'q}_{\eta,\alpha\alpha}(k',k)\\ &\times\delta\left[\mathcal{E}^{\alpha}_{q+\Phi_\rho}(k)-\mathcal{E}^{\alpha}_{q'+\Phi_\rho}(k')\right]\\ &\times\left[\mathrm{sgn}[v^{\alpha}_{q+\Phi_\rho}(k)]\mathrm{sgn}[v^{\alpha}_{q'+\Phi_\rho}(k')]-1\right]\\ &\times\left\{\delta\left[\mathcal{E}_F(0)-\mathcal{E}^{\alpha}_{q+\Phi_\rho}(k)-\frac{eV_{sd}}{2}\mathrm{sgn}[v^{\alpha}_{q+\Phi_\rho}(k)]\right]\right.\\ &\left.+\delta\left[\mathcal{E}_F(0)-\mathcal{E}^{\alpha}_{q'+\Phi_\rho}(k')-\frac{eV_{sd}}{2}\mathrm{sgn}[v^{\alpha}_{q'+\Phi_\rho}(k')]\right]\right\},\end{aligned} \tag{6}$$

where $G^{\alpha\alpha}_{total,imp} = G^{++}_{imp} + G^{--}_{imp}$. Also, $v^{\pm}_{q+\Phi_\rho}(k) = (1/\hbar)\partial\mathcal{E}^{\pm}_{q+\Phi_\rho}(k)/\partial k$ is the electron velocity and $J^{qq'}_{\xi,\alpha\beta}(k,k')$ is a matrix for the impurity potential located at a position, namely, $\vec{x}_\xi$ [44]. We have also assumed that the magnetic field does not affect the Fermi energy, i.e. $\mathcal{E}_F(B) = \mathcal{E}_F(0)$. More importantly, the expression $[\mathrm{sgn}[v^{\alpha}_{q+\Phi_\rho}(k)]\mathrm{sgn}[v^{\alpha}_{q'+\Phi_\rho}(k')]-1]$ controls the scattering event from the initial state to the final state via the sign of the electron velocity. It requires that only backward scattering events are possible in one-dimensional systems like nanotubes. The coherent backscattering (CBS) of the electron is an effect that describes the appearance of a backscattered peak when the electron traveling in a time-reversed path self-interferes constructively in the backscattered direction. This means that the electronic wave is weakly localized [50–52].

By obtaining the solutions of the energy–momentum conservation equation, i.e. $\mathcal{E}^{\alpha}_{q+\Phi_\rho}(k) = \mathcal{E}^{\alpha}_{q'+\Phi_\rho}(k+\mathbf{g})$ where

g is the transferred momentum, we now evaluate equation (6) at some special k-points in the FBZ. Using equation (3) for the (n, n) armchair nanotubes one obtains

$$\mathbf{g}^{\pm} = -k \pm \frac{2}{\sqrt{3}a_{cc}} \arccos\left\{-\frac{1}{2}\cos\left(\frac{3(q'+\Phi_\rho)a_{cc}}{2r_t}\right) \pm \frac{1}{2}\left[\cos^2\left(\frac{3(q'+\Phi_\rho)a_{cc}}{2r_t}\right) + 4\cos^2\left(\frac{\sqrt{3}ka_{cc}}{2}\right) + 4\cos\left(\frac{\sqrt{3}ka_{cc}}{2}\right)\cos\left(\frac{3(q+\Phi_\rho)a_{cc}}{2r_t}\right)\right]^{\frac{1}{2}}\right\}, \quad (7)$$

and for the $(n, 0)$ zigzag nanotubes the equivalent expression is given by

$$\mathbf{g}^{\pm} = -k \pm \frac{2}{3a_{cc}} \arccos\left\{\frac{1}{\cos\left(\frac{\sqrt{3}(q'+\Phi_\rho)a_{cc}}{2r_t}\right)} \times \left[-\cos^2\left(\frac{\sqrt{3}(q'+\Phi_\rho)a_{cc}}{2r_t}\right) + \cos^2\left(\frac{\sqrt{3}(q+\Phi_\rho)a_{cc}}{2r_t}\right) + \cos\left(\frac{\sqrt{3}(q+\Phi_\rho)a_{cc}}{2r_t}\right)\cos\left(\frac{3ka_{cc}}{2}\right)\right]\right\}. \quad (8)$$

For the intrasubband scattering, i.e. $|q + \Phi_\rho, k\rangle \rightarrow |q' + \Phi_\rho, k'\rangle = |q + \Phi_\rho, k + \mathbf{g}\rangle$, equation (7) has four scattering roots as follows:

$$\mathbf{g}^{\pm} = 0,\quad -2k,\quad -k \pm \frac{2}{\sqrt{3}a_{cc}} \arccos\left[\cos\left(\frac{3(q+\Phi_\rho)a_{cc}}{2r_t}\right) + \cos\left(\frac{\sqrt{3}ka_{cc}}{2}\right)\right], \quad (9)$$

while for the metallic zigzag nanotubes equation (8) provides only two roots 0 and $-2k$.

$k' = k$: The root $\mathbf{g}^{\pm} = 0$ means that q and k are conserved, and no scattering event has occurred. Thus, the MDC becomes zero.

$k' = -k$: The root $\mathbf{g}^{\pm} = -2k$ describes the CBS of the electron within the same subband to another Fermi point. In the CBS effect, the electron is elastically scattered back to a momentum directly opposite to its original momentum state in the momentum space. Let G_{imp} be replaced later on by G_{CBS}. For a *couple* of impurities located at $\vec{x}_\xi = \vec{T}_{l_1} + \vec{R}_{j_1} + \vec{d}_1$ and $\vec{x}_\eta = \vec{T}_{l_2} + \vec{R}_{j_2} + \vec{d}_2$, equation (6) yields [44]

$$\mathrm{Re}\left(\frac{G^{\alpha\alpha}_{CBS}[V_{sd}, \mathcal{E}_F(0), \Phi_\rho]}{G_0}\right) = e|V_{sd}|\left(\frac{\pi g}{2\mathcal{M}\mathcal{N}}\right)^2 \times \sum_{q=1}^{N_t/2}\sum_{k\in}^{FBZ}\delta\left\{\left[\mathcal{E}_F(0) - \mathcal{E}^{\alpha}_{q+\Phi_\rho}(k)\right]^2 - \left[\frac{eV_{sd}}{2}\right]^2\right\} \times \cos\left\{2k\left[(l_2 - l_1)T + \left(\vec{R}_{j_2} - \vec{R}_{j_1}\right)\cdot\frac{\vec{T}}{T}\right]\right\}, \quad (10)$$

where $\mathcal{M}$ is the total number of nanotube unit cells [44]. Because $\mathcal{E}^{+}_{q+\Phi_\rho}(k) = -\mathcal{E}^{-}_{q+\Phi_\rho}(k)$; if $\mathcal{E}_F(0) = 0$ then $G^{++}_{CBS} = G^{--}_{CBS}$. For the case of a *single* impurity the CBSIP is destroyed. Because two carbon atoms A and B inside a graphite unit cell belong to two different sublattices, the impurity can occupy one of the lattice site. For simplicity, we have here assumed that two impurities are substituted on B-sites with the same circumferential angle along the nanotube axis [44]. These arrangements of impurities break all mirror symmetry planes containing the nanotube axis [16]. By turning the sum over k into an integral and exploiting equation (5) for the lowest lying subband, equation (10) leads to

$$\mathrm{Re}\left(\frac{G^{\alpha\alpha}_{CBS}[V_{sd}, \Phi_\rho]}{G_0}\right) = \left(\frac{\pi e V_{sd} g^2 T^Y}{X\hbar^2 v_F^2 \mathcal{M}\mathcal{N}_Y^2}\right) \times \left[\left(\frac{eV_{sd}}{\hbar v_F}\right)^2 - \left(\frac{\Phi^Y_\rho}{r^Y_t}\right)^2\right]^{-\frac{1}{2}} \times \cos\left[2k_F(l_2 - l_1)T^Y\right] \times \cos\left[\sqrt{\left(\frac{eV_{sd}}{\hbar v_F}\right)^2 - \left(\frac{\Phi^Y_\rho}{r^Y_t}\right)^2}\,(l_2 - l_1)T^Y\right]. \quad (11)$$

The total DC is then $\mathrm{Re}[G^{tot,Y}_{CBS}] = 2\,\mathrm{Re}[G^{++,Y}_{CBS}] = 2\,\mathrm{Re}[G^{--,Y}_{CBS}]$. From equation (11) one can draw several conclusions: (1) For the armchair nanotubes we have $X = 1$, $Y =$ arm, and $k_F = 2\pi/3T^{arm}$, while for the metallic zigzag ones $X = 2$, $Y = zig$, and $k_F = 0$. (2) The cosine term is responsible for the CBSIP. Averaging over different impurity configurations melts away this interference term. (3) No switching effect from positive to negative MDC occurs by changing the orientation of the magnetic field with respect to the nanotube axis. This means that, the reciprocity relation $G_{CBS}(\Phi_\rho) = G_{CBS}(-\Phi_\rho)$ is fulfilled. (4) The amplitude of this CBSIP depends on both the source–drain voltage and the AB-flux. (5) In the limit $\Phi_\rho \rightarrow 0$ one recovers the solution of the free-magnetic field case derived in [44]. (6) Conduction through this gapped nanotube is sensitively dependent on the exact position of the V_{sd} with respect to the lowest level subband edges. Strictly speaking, there is a threshold voltage determined by $eV_{sd} \geqslant 3\Delta_0\Phi_\rho/2$ and $eV_{sd} \leqslant -3\Delta_0\Phi_\rho/2$ below and above which, respectively, the transport is forbidden. This issue is in agreement with the density of state due to the one-dimensional subbands expected for semiconductor nanotubes. In other words, the MDC is singular at the position of the lowest subband bottom indicating its van Hove singularity. (7) A closer look at the argument of the second cosine term reveals that the interference term leads to aperiodic oscillations in the MDC profile. This is because this argument is a nonlinear mapping of the AB-flux as well as the source–drain voltage. In fact, the DC is aperiodically modulated through the AB-flux. At zero temperature, it would be plausible if we suppose that the system size plays the role of the phase coherence length. In the presence of the AB-flux the electrons acquire additional phases, and we can control the interference pattern made from the conjugated time-reversed paths. The negative MDC is more important. Actually, it originates from not only the QI effects but also the pseudospin conservation rule. The negative MDC feature may be exploited for designing magneto-conductance switches based on the AB effect.

$k' = \pm(2/\sqrt{3}a_{cc})\arccos[\cos(3(q + \Phi_\rho)a_{cc}/2r_t) + \cos(\sqrt{3}ka_{cc}/2)]$: These two last roots are actually the intersubband backscattering around the same Fermi point, and we currently discard them [56].

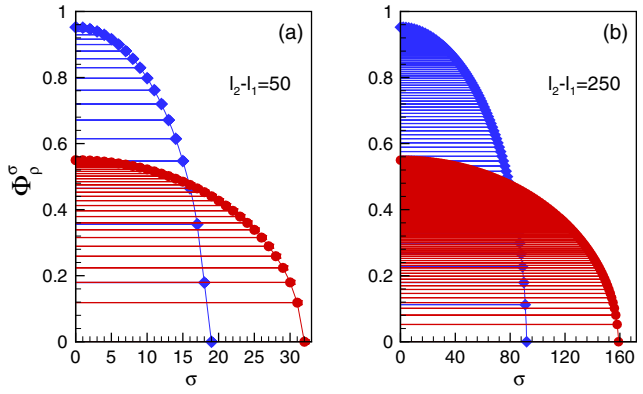

Figure 2. The positions of extrema in Φ_ρ-space are calculated using the upper part of equation (14). (a) The allowed σ's for the (6, 6) (diamond, blue) and (6, 0) (circle, red) nanotubes, with $l_2 - l_1 = 50$ and $eV_{sd} = 0.11$, are 18 and 33, respectively. (b) The allowed σ's for the (6, 6) (diamond, blue) and (6, 0) (circle, red) nanotubes, with $l_2 - l_1 = 250$ and $eV_{sd} = 0.11$, are 93 and 160, respectively. The spacing between two horizontally adjacent lines is decreased with increasing magnetic field, which obviously shows that oscillations are aperiodic.

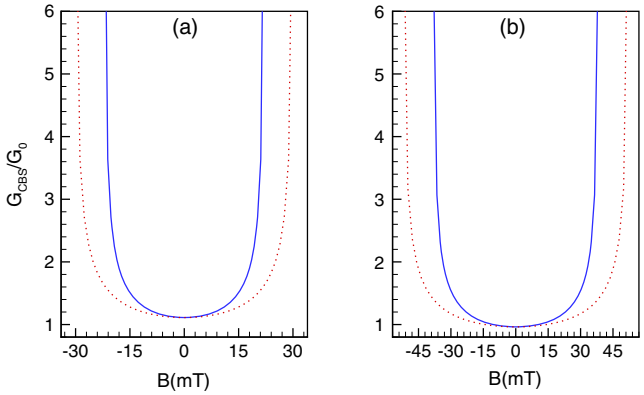

Figure 3. Calculated MDC as a function of the magnetic field B for a single impurity. Results come from evaluating equation (11) for the armchair and metallic zigzag nanotubes. (a) Traces are plotted for the (6, 6) armchair, with $eV_{sd} = 0.11$ and $B \in [-22, 22]$ mT (solid, blue), and $eV_{sd} = 0.15$ with $B \in [-30, 30]$ mT (dotted, red). (b) Traces are plotted for the (6, 0) zigzag, with $eV_{sd} = 0.11$ and $B \in [-38, 38]$ mT (solid, blue), and $eV_{sd} = 0.15$ with $B \in [-52, 52]$ mT (dotted, red). They exhibit a U-like behavior. The plateau of the zigzag nanotube is approximately twice the plateau of the armchair one.

3. Discussions

Using the two-terminal Landauer–Bütticker approach for a two-band model, the whole resistance of the nanotube is approximately given by [12]

$$G_{\rm tube}^{-1} = (G_{\rm perfect})^{-1} + G_{\rm CBS}^{-1} + G_{c1}^{-1} + G_{c2}^{-1}. \qquad (12)$$

In the above equation, the first term is the resistance of a perfect ballistic nanotube with perfect contacts. It originates from the redistribution of electrons between reservoirs and the nanotube. The second term is the quantum correction coming from the CBS effect. Two last terms, discarded here, are for imperfect contacts between the nanotube and reservoirs. To investigate the behavior of the MDC as a function of the AB-flux, we have numerically performed equation (11) for both armchair and zigzag nanotubes. Results are the same for both repulsive and attractive impurity potentials. Let us suppose $g = 10^4\gamma_0$, representing a typical impurity, and $\mathcal{M} = 1000\,000$. In equation (11), the product of two cosine terms is actually a resultant wave coming from the superposition of two standing waves with the same amplitude but different wavenumbers $k_1 = k_{\rm F} + (1/2)\sqrt{(eV_{\rm sd}/\hbar v_{\rm F})^2 - (\Phi_\rho/r_t)^2}$ and $k_2 = k_{\rm F} - (1/2)\sqrt{(eV_{\rm sd}/\hbar v_{\rm F})^2 - (\Phi_\rho/r_t)^2}$. These two initial standing waves describing two degenerate resonant states induced by impurities in the FBZ are given by

$$f_i = \left(\frac{\pi e V_{\rm sd} g^2 T}{2X\hbar^2 v_{\rm F}^2 \mathcal{M}\mathcal{N}^2}\right)\left[\left(\frac{eV_{\rm sd}}{\hbar v_{\rm F}}\right)^2 - \left(\frac{\Phi_\rho}{r_t}\right)^2\right]^{-\frac{1}{2}} \times \cos(2k_i l_{\rm m}), \quad i = 1, 2. \qquad (13)$$

Because two functions f_1 and f_2 are not periodic in the Φ_ρ-space, neither is their superposition, i.e. $f_1 + f_2$. Thus, an aperiodic variation in the MDC is expected. The phase difference for an electron propagating over the length $l_{\rm m}$ is given by $\delta\varphi(\Phi_\rho) = 2\Delta k l_{\rm m}$ where $\Delta k = k_1 - k_2 = \sqrt{(eV_{\rm sd}/\hbar v_{\rm F})^2 - (\Phi_\rho/r_t)^2}$. Constructive interference occurs when the extrema of two waves add together and the phase difference becomes an integer multiple of π, i.e. $\delta\varphi(\Phi_\rho) = \sigma\pi$, with $\sigma \in \mathbb{Z}$. On the other hand, destructive interference occurs when two waves have a phase difference of a half-integer multiple of π, i.e. $\delta\varphi(\Phi_\rho) = (\sigma + 1/2)\pi$. An analytic expression in the Φ_ρ-space can be derived easily as follows:

$$\Phi_\rho^\sigma = \begin{cases} \pm r_t\left[\left(\dfrac{eV_{\rm sd}}{\hbar v_{\rm F}}\right)^2 - \left(\dfrac{\sigma\pi}{2l_{\rm m}}\right)^2\right]^{\frac{1}{2}}, \\ \qquad \text{constructive} \\ \pm r_t\left[\left(\dfrac{eV_{\rm sd}}{\hbar v_{\rm F}}\right)^2 - \left(\dfrac{(2\sigma+1)\pi}{2l_{\rm m}}\right)^2\right]^{\frac{1}{2}}, \\ \qquad \text{destructive.} \end{cases} \qquad (14)$$

The above equation actually gives the spacing between the MDC extrema (constructive) or zeros (destructive) in the Φ_ρ-space. Due to the nonlinear mapping between $\delta\varphi(\Phi_\rho)$ and Φ_ρ, the MDC versus Φ_ρ behaves aperiodically. The most important feature is that extrema and zeros are located at *irrational fractions* in Φ_ρ-space. In other words, Φ = irrational $\times$ Φ_0. The nonlinear dependence of the extrema positions as a function of σ is depicted in figures 2(a) and (b) for $l_2 - l_1 = 50$ and 250, respectively. In both panels the nonlinear behavior of oscillations can be seen by comparing the spacing between two horizontally adjacent lines. It should be pointed out that variations in the MDC are aperiodic in $eV_{\rm sd}$-space as well.

Also, Δk can be expressed in terms of the series $\Delta k = \lambda(1 + \chi/2 - \chi^2/8 + \chi^3/16 - \cdots)$, where $\lambda = |eV_{\rm sd}/\hbar v_{\rm F}|$ and $\chi(\Phi_\rho) = -(\Phi_\rho/r_t)^2/(eV_{\rm sd}/\hbar v_{\rm F})^2$. Thus, the phase accumulated by the electron can be expressed by $\delta\varphi = \delta\varphi(0) + \delta\varphi(\Phi_\rho)$, where $\delta\varphi(0) = 2\lambda l_{\rm m}$ is the phase difference in the absence of the AB-flux and $\delta\varphi(\Phi_\rho) = \lambda l_{\rm m}(\chi - \chi^2/4 + \chi^3/8 -$

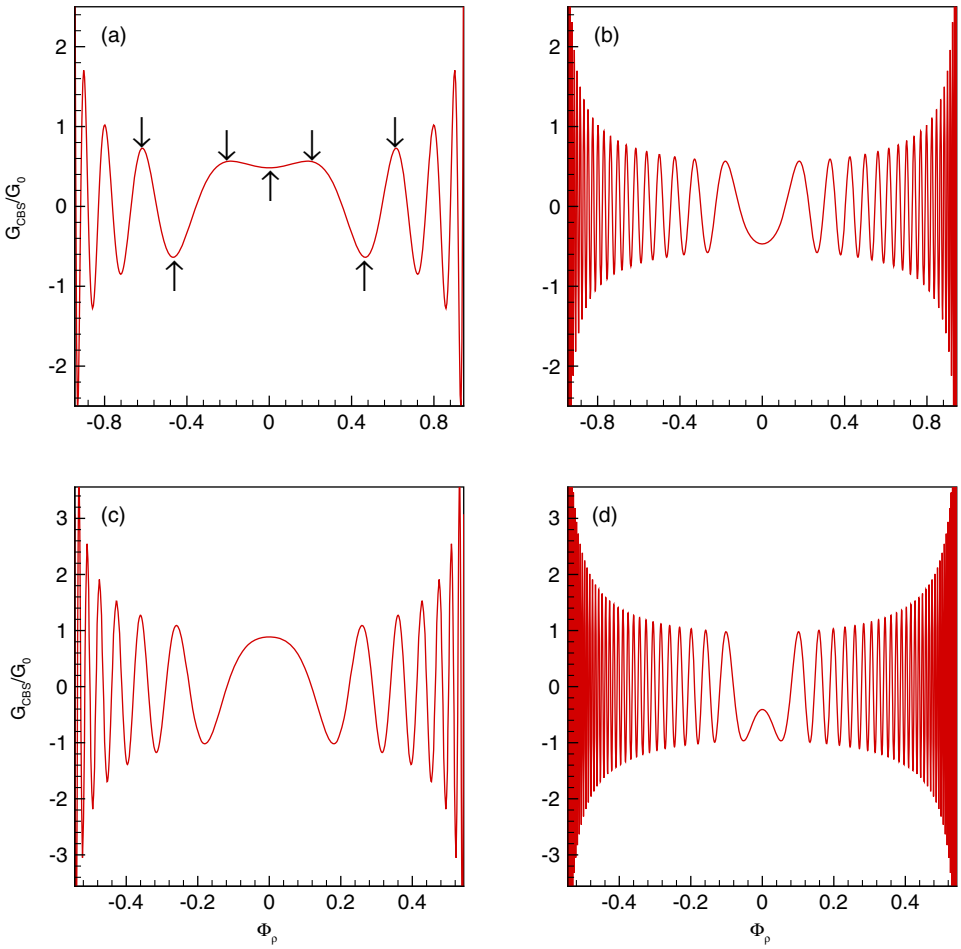

Figure 4. The calculated MDC coming from evaluating equation (11) for the nanotube (n, m) for a pair of impurities. The CBSIP shows aperiodic oscillations. The extrema as well as zeros are located at the irrational fractions of Φ_ρ. Positions of some extrema are indicated by arrows. (a) $(n, m) = (6, 6)$, $eV_{sd} = 0.11$, $B \in [-22, 22]$ (mT), and $l_2 - l_1 = 50$; (b) $(n, m) = (6, 6)$, $eV_{sd} = 0.11$, $B \in [-22, 22]$ (mT), and $l_2 - l_1 = 250$; (c) $(n, m) = (6, 0)$, $eV_{sd} = 0.11$, $B \in [-38, 38]$ (mT), and $l_2 - l_1 = 50$; (d) $(n, m) = (6, 0)$, $eV_{sd} = 0.11$, $B \in [-38, 38]$ (mT), and $l_2 - l_1 = 250$. A comparison between, say, panels (b) and (d), exhibits that the faster/higher and slower/shorter aperiodic fluctuations belong to metallic zigzag and armchair nanotubes, respectively.

$\cdots$) is the magnetic field dependent phase difference. As a check, we see that, for $\chi = 0$, i.e. in the absence of the AB-flux, $\delta\varphi(\Phi_\rho) = 0$. For the (n, n) armchair and $(n, 0)$ zigzag nanotubes we find $r_t^{arm} = 3na_{cc}/2\pi$; $T^{arm} = \sqrt{3}a_{cc}$, and $r_t^{zig} = \sqrt{3}na_{cc}/2\pi$; $T^{zig} = 3a_{cc}$, respectively, so in this case we approximate $\delta\varphi(\Phi_\rho)$ by $\lambda l_m \chi$ and it is straightforward to show that $\delta\varphi(\Phi_\rho)^{arm}/\delta\varphi(\Phi_\rho)^{zig} = \sqrt{3}$.

For a single impurity where $l_2 = l_1$, the nanotube is less defective. In this case the quantum interference due to the CBS is destroyed and the AB modulation becomes dominant. Evaluating equation (11) leads to a U-like behavior for the armchair and zigzag nanotubes. As depicted in figure 3, these curves are symmetric and centered at $B = 0$ (or $\Phi_\rho = 0$). Each curve has a plateau which decreases with increasing magnetic field and its magnitude depends strongly on the location of the source–drain voltage. A detailed look at panels 3(a) and (b) shows that the magnitude of the zigzag plateau is approximately twice the armchair one for a fixed value of the source–drain voltage. Recently, Lassagne *et al* [40] have also observed such U-like curves, of course through a Schottky barrier for different gate voltages at non-zero temperatures, for a clean multiwalled nanotube threaded by an AB-flux. We should emphasize that although our result share some similarities in the AB-pattern with that of [40] their underlying physical transport phenomena could be different. It is expected that at a non-zero temperature and gate voltage such U-like behavior would drastically changed in our model.

Moreover, for a couple of impurities, with $l_1 \neq l_2$, the MDC as a function of Φ_ρ for two different distances between impurities is calculated. In figure 4, panels show aperiodic fluctuations which alter between positive and negative values. The amplitude of oscillations is increased with increasing magnetic field, while the spacing between two adjacent extrema is decreased. These fluctuations represent a hallmark of defective quantum transport resulting from competition between the CBS effect and the AB-flux. Such fluctuations may be attributed to the Fabry–Perot oscillations [53] modulated by the AB-flux. The positions of some extrema in the MDC are labeled by arrows in figure 4(a). The most striking and immediately visible difference between armchair oscillations and zigzag ones, say by comparing panels 4(b)

and (d), is that for the same value of the source–drain voltage the fluctuations of the zigzag nanotubes are faster and higher than those of the armchair one. The envelope functions of the extrema have a U-shaped appearance as well.

In summary, this semi-classical study shows the subtle interplay between the quantum interference phenomena originating from Fabry–Perot oscillations [53] and the magnetic field dependence of the band structure in defective metallic nanotubes. We have shown how such oscillations can be modulated using the AB-flux. Nonlinear mapping between the MDC and the magnetic filed leads to aperiodic fluctuations. Such results may be applied for manipulating defective metallic nanotubes into quantum interference devices, say, for the construction of nanotube magneto-conductance devices based on the AB effect [55]. Moreover, it is worth mentioning that the model is flexible enough to incorporate inelastic events like electron–electron and electron–phonon scattering events. In the presence of such decoherent effects we expect a drastic change in the interference pattern of the differential conductance.

Acknowledgment

The author would like to acknowledge Professor Stephan Roche for reading the manuscript, and suggesting effective and critical points.

References

[1] Charlier J C, Blase X and Roche S 2007 *Rev. Mod. Phys.* **79** 677
[2] Saito R, Dresslhuas G and Dresslhaus M S 1998 *Physical Properties of Carbon Nanotubes* (London: Imperial College Press)
[3] Mintmire J W, Dunlap B I and White C T 1992 *Phys. Rev. Lett.* **68** 631
[4] Hamada N, Sawada S I and Oshiyama A 1992 *Phys. Rev. Lett.* **68** 1579
[5] Dekker C 1999 *Phys. Today* **52** (5) 22
[6] White C T and Todorov T N 1998 *Nature* **393** 240
[7] Tans S, Devoret M H, Dai H, Thess A, Smalley R E, Geerligs L J and Dekker C 1997 *Nature* **386** 474
[8] Bockrath M, Cobden D H, McEuen P L, Chopra N G, Zettl A, Thess A and Smalley R E 1997 *Science* **275** 1922
[9] Tans S, Verschueren A R M and Dekker C 1998 *Nature* **393** 49
[10] Tsukagoshi K, Alphenaar B W and Ago H 1999 *Nature* **401** 572
[11] Landauer R 1970 *Phil. Mag.* **21** 863
[12] Datta S 1995 *Electronic Transport in Mesoscopic Systems* (Cambridge: Cambridge University Press)
[13] Frank S, Poncharal P, Wang Z L and de Heer W A 1998 *Science* **280** 1744
[14] Nardelli M B 1999 *Phys. Rev.* B **60** 7828
Nardelli M B and Bernholc J 1999 *Phys. Rev.* B **60** 16338
[15] Chico L, Benedict L X, Louie S G and Cohen M L 1996 *Phys. Rev.* B **54** 2600
[16] Song H-F, Zhu J-L and Xiong J-J 2002 *Phys. Rev.* B **65** 085408
[17] Anantram M P and Govindan T R 1998 *Phys. Rev.* B **58** 4882
[18] Ando T and Nakanishi T 1998 *J. Phys. Soc. Japan* **67** 1704
Ando T, Nakanishi T and Saito R 1998 *J. Phys. Soc. Japan* **67** 2857
[19] Roche S, Triozon F and Rubio A 2001 *Appl. Phys. Lett.* **79** 3690
[20] Liu Y and Guo H 2004 *Phys. Rev.* B **69** 115401
[21] Lee R S, Kim H J, Fischer J E, Thess A and Smalley R 1997 *Nature* **388** 255
[22] Yao Z, Postma H W Ch, Balents L and Dekker C 1999 *Nature* **402** 273
[23] Bochrath M, Liang W, Bozovic D, Hafner J H, Lieber C H, Tinkham M and Park H 2001 *Science* **291** 283
[24] Collins P G, Zettl A, Bando H, Thess A and Smalley R E 1997 *Science* **278** 100
[25] Stone A J and Wales D J 1986 *Chem. Phys. Lett.* **128** 501
[26] Bergmann G 1984 *Phys. Rep.* **107** 1
[27] Aronov A G and Sharvin Y V 1987 *Rev. Mod. Phys.* **59** 755
[28] Altshuler B L, Aronov A G, Spivak B Z, Sharvin D Yu and Sharvin Yu V 1982 *JETP Lett.* **35** 588
[29] Ludwig T and Mirlin A D 2004 *Phys. Rev.* B **69** 193306
[30] Ajiki H and Ando T 1993 *J. Phys. Soc. Japan* **62** 1255
[31] Roche S, Dresslhuas G, Dresslhuas M S and Saito R 2000 *Phys. Rev.* B **62** 16092
[32] Bachtold A, Strunk C, Salvetat J-P, Bonard J-M, Forró L, Nussbaumer T and Schönenberger C 1999 *Nature* **397** 673
[33] Tian W and Datta S 1994 *Phys. Rev.* B **4** 5097
[34] Lassagne B, Raquet B, Broto J M and González J 2006 *J. Phys.: Condens. Matter* **18** 4581
[35] Fedorov G, Lassagne B, Sagnes M, Raquet B, Broto J-M, Triozon F, Roche S and Flahaut E 2005 *Phys. Rev. Lett.* **94** 066801
[36] Stojetz B, Miko C, Forró L and Strunk C 2005 *Phys. Rev. Lett.* **94** 186802
[37] Zaric S, Ostojic G N, Kono J, Shaver J, Moore V C, Strano M S, Hauge R H, Smalley R E and Wei X 2004 *Science* **304** 1129
[38] Coskun U C, Wei T-C, Vishveshwara S, Goldbart P M and Bezryadin A 2004 *Science* **304** 1132
[39] Minot E D, Yaish Y, Sazonova V and McEuen P L 2004 *Nature* **428** 536
[40] Lassagne B, Cleuziou J-P, Nanot S, Escoffier W, Avriller R, Roche S, Forró L, Raquet B and Broto J-M 2007 *Phys. Rev. Lett.* **98** 176802
[41] Strunk C, Stojetz B and Roche S 2006 *Semicond. Sci. Technol.* **21** S38–45
[42] Lu J P 1995 *Phys. Rev. Lett.* **74** 1123
[43] O'Connell M (ed) 2006 *Carbon Nanotubes: Properties and Applications* (London: Taylor and Francis) (Boca Raton, FL: CRC Press)
[44] Bagheri M and Namiranian A 2007 *J. Phys.: Condens. Matter* **19** 096207
[45] Aharonov Y and Bohm D 1959 *Phys. Rev.* **115** 485
[46] Mahan G D 2004 *Phys. Rev.* B **69** 125407
[47] Kulik I O 1967 *JETP Lett.* **5** 345
[48] Kulik I O, Omelyanchouk A N and Tuluzov I G 1988 *Sov. J. Low. Temp. Phys.* **14** 149
[49] Namiranian A 2004 *Phys. Rev.* B **70** 073402
[50] Bruus H and Flensberg K 2004 *Many-body Quantum Theory in Condensed Matter Physics* (New York: Oxford University Press)
[51] Suzuura H and Ando T 2006 *J. Phys. Soc. Japan* **75** 024703
[52] McCann E, Kechedzhi K, Falko V I, Suzuura H, Ando T and Altshuler B L 2006 *Phys. Rev. Lett.* **97** 146805
[53] Liang W, Bockrath M, Bozovic D, Hafner J H, Tinkham M and Park H 2001 *Nature* **411** 665
[54] Jiang J, Dong J and Xing D Y 2003 *Phys. Rev. Lett.* **91** 056802
[55] Hod O, Rabani E and Baer R 2005 *J. Chem. Phys.* **123** 051103
[56] Petrov A G and Rotkin S V 2004 *Phys. Rev.* B **70** 035408